

# Estimation of Inlet Flow Rates for Image-Based Aneurysm CFD Models: Where and How to Begin?

KRISTIAN VALEN-SENDSTAD,<sup>1,2</sup> MARINA PICCINELLI,<sup>3</sup> RESMI KRISHNANKUTTYREMA,<sup>1,4</sup>  
and DAVID. A. STEINMAN<sup>1,4</sup>

<sup>1</sup>Biomedical Simulation Laboratory, Department of Mechanical & Industrial Engineering, University of Toronto, 5 King's College Road, Toronto ON M5S 3G8, Canada; <sup>2</sup>Center for Biomedical Computing, Simula Research Laboratory, Lysaker, Norway; <sup>3</sup>Department of Radiology & Imaging Sciences, Emory University, Atlanta, GA, USA; and <sup>4</sup>Institute of Biomaterials & Biomedical Engineering, University of Toronto, Toronto, Canada

(Received 12 December 2014; accepted 19 February 2015; published online 24 February 2015)

Associate Editor Diego Gallo oversaw the review of this article.

**Abstract**—Patient-specific flow rates are rarely available for image-based computational fluid dynamics models. Instead, flow rates are often assumed to scale according to the diameters of the arteries of interest. Our goal was to determine how choice of inlet location and scaling law affect such model-based estimation of inflow rates. We focused on 37 internal carotid artery (ICA) aneurysm cases from the Aneurisk cohort. An average ICA flow rate of  $245 \text{ mL min}^{-1}$  was assumed from the literature, and then rescaled for each case according to its inlet diameter squared (assuming a fixed velocity) or cubed (assuming a fixed wall shear stress). Scaling was based on diameters measured at various consistent anatomical locations along the models. Choice of location introduced a modest 17% average uncertainty in model-based flow rate, but within individual cases estimated flow rates could vary by  $>100 \text{ mL min}^{-1}$ . A square law was found to be more consistent with physiological flow rates than a cube law. Although impact of parent artery truncation on downstream flow patterns is well studied, our study highlights a more insidious and potentially equal impact of truncation site and scaling law on the uncertainty of assumed inlet flow rates and thus, potentially, downstream flow patterns.

**Keywords**—Volumetric flow rate, Intracranial aneurysm, Aneurysm rupture, Neuroradiology, Scaling law, Cube law, Inlet truncation.

## INTRODUCTION

The combination of medical imaging and computational fluid dynamics (CFD) has become an essential tool for studying arterial hemodynamics and their impact on vascular pathologies and therapies. Yet, while patient-specific lumen geometries are readily available from routine clinical angiography,<sup>33</sup> only relatively rarely are patient-specific velocity<sup>24,37</sup> or flow rate boundary conditions<sup>11,15</sup> acquired. The simplest alternative is to apply a typical flow rate from the literature; however, this overlooks natural variations in flow rate among individuals. It is well known, for example, that flow rates can depend on demographic factors like age or sex, body size, normal or pathological variants of vascular anatomy, presence of contralateral disease, *etc.* These factors may be invisible to the CFD modeler, but even if known there is not necessarily a simple relationship between them and flow rate.

A common alternative is to exploit the principle that vessel diameter can be a reflection of the flow rate. For example, it has been demonstrated that vessels adapt their caliber to maintain the prevailing wall shear stress (WSS),<sup>18</sup> which under the assumption of Poiseuille flow implies that blood flow rate scales with the cube of the lumen diameter (i.e.,  $Q \sim D^3$ ), consistent with Murray's eponymous cube law for bifurcation flow splitting.<sup>25</sup> On the other hand, Zamir<sup>41</sup> showed that bifurcations of the larger, conduit arteries more closely obey a square law (i.e.,  $Q \sim D^2$ ), owing to the presence of more complicated blood flow dynamics. A square law for larger arteries has also been deduced from inter- and intra-species WSS measurements<sup>8,32</sup> or derived from allometric scaling principles.<sup>38</sup> In short, demographic,

---

Address correspondence to David. A. Steinman, Biomedical Simulation Laboratory, Department of Mechanical & Industrial Engineering, University of Toronto, 5 King's College Road, Toronto ON M5S 3G8, Canada. Electronic mail: steinman@mie.utoronto.ca

anatomical or physiological factors driving the demand for blood flow through a particular vessel may be effectively encoded in the vessel size, at least approximately.

Assuming the validity of such flow-diameter scaling laws, estimation of an individual's flow rate then boils down to measurement of the lumen diameter. In practice, however, the choice of diameter measurement location is often dictated by the truncation of the CFD model at some point upstream of the site of interest. Even for 'full-length' models, lumen diameters may naturally vary along the length,<sup>31</sup> begging the question of where to apply the scaling law. Diameter measurements are also subject to uncertainties owing to noise in the source images and/or the resulting lumen segmentation. While previous studies have investigated the impact of inlet length truncation on flow patterns at aneurysms<sup>4,10,21,27</sup> or elsewhere,<sup>12</sup> they have typically fixed the flow rate for each case, irrespective of the imposed variations in truncation site and consequently inlet diameter, instead focusing on the impact of change in upstream velocity profile shape on the downstream flow patterns.

The aim of this study was to understand how the choice of diameter measurement location and power law model might affect the estimation of inflow rates for a cohort of image-based CFD models. Here we focused on what is arguably the most straightforward scenario: the internal carotid artery (ICA). For one, mean flow in the cerebrovasculature is well regulated, and thus relatively immune to changes in physiological state.<sup>3</sup> Also, the ICA has few and relatively small side branches, meaning that flow is mostly conserved along its length. Finally, the ICA is a common site for intracranial aneurysm formation, and recent evidence suggests the need to incorporate the ICA into CFD models even for downstream MCA aneurysms.<sup>35</sup>

## MATERIALS AND METHODS

### *Study Group*

We focused on ICA sidewall aneurysm cases from the online Aneurisk dataset repository (<http://ecm2.mathcs.emory.edu/aneurisk>). Cases were included only if they extended upstream at least to the cavernous (C4) segment of the ICA, which resulted in  $N = 37$  cases, of which a representative selection is shown in Fig. 1. Demographics for these cases were: age  $55 \pm 15$  years (range 26–85); 86% female; 73% ruptured. Further details about the Aneurisk cohort, and about the digital segmentation and geometric analysis, are provided elsewhere.<sup>28</sup> Use of these data in the

Aneurisk repository has been authorized by the Ethical Committee of the Ca' Granda Niguarda Hospital.

### *Flow Rate Scaling*

The inlet flow rate ( $Q$ ) was assumed to scale with diameter ( $D$ ) according to a general power law model, i.e.,  $Q \sim D^n$ . To determine the effective constant of proportionality, we followed the approach of Lee *et al.*<sup>19</sup> i.e.:

$$Q_i = Q_{\text{avg}} \times \frac{D_i^n}{D_{\text{avg}}^n}$$

where  $D_i$  and  $Q_i$  are, respectively, the (measured) individual diameter and the (to-be-estimated) individual flow rate. For a given diameter measurement location, the population average,  $D_{\text{avg}}^n$ , was approximated as the average of  $D_i^n$ . This ensures that the average value of the estimated  $Q$  for a given measurement location is identically  $Q_{\text{avg}}$ . The age range of our cohort suggested the use of an average *older adult* mean ICA flow rate, so we chose  $Q_{\text{avg}} = 245 \text{ mL min}^{-1}$  based on an independent study of 94 older adults.<sup>13</sup> That study found no significant difference between male and female ICA flow rates, and so like the vast majority of image-based CFD studies we did not account for sex into flow rate calculations. We considered two different power law exponents:  $n = 2$ , implying that flow rate scales with cross-sectional area, i.e., same inflow velocity ( $V$ ) for all cases (e.g., Valen-Sendstad and Steinman<sup>36</sup>); and  $n = 3$ , which is tantamount to assuming the same inlet wall shear stress (WSS) for all cases (e.g., Cebra *et al.*<sup>7</sup>). As discussed later, we did not consider pulsatility, and so focused only on the estimation of cycle-averaged flow rate.

### *Diameter Measurement*

The vast majority of image-based CFD studies appear to truncate their inlets opportunistically, i.e., as far upstream as the operator can (or wishes to) segment the lumen from the medical images. We refer to this location as the 'Inlet'. Conversely, the parent artery may be truncated close to the aneurysm, owing to a lack of coverage or a desire to minimize the computational domain and effort. Following Piccinelli *et al.*<sup>29</sup> we defined this 'Clip' location objectively and automatically as being one diameter proximal to the aneurysm neck.

In between these extremes we defined a set of consistent anatomical locations at which the diameters of all cases could be rationally compared. As shown in Fig. 1, these corresponded to the transition points (i.e., proximal ends) of the various bends of the ICA

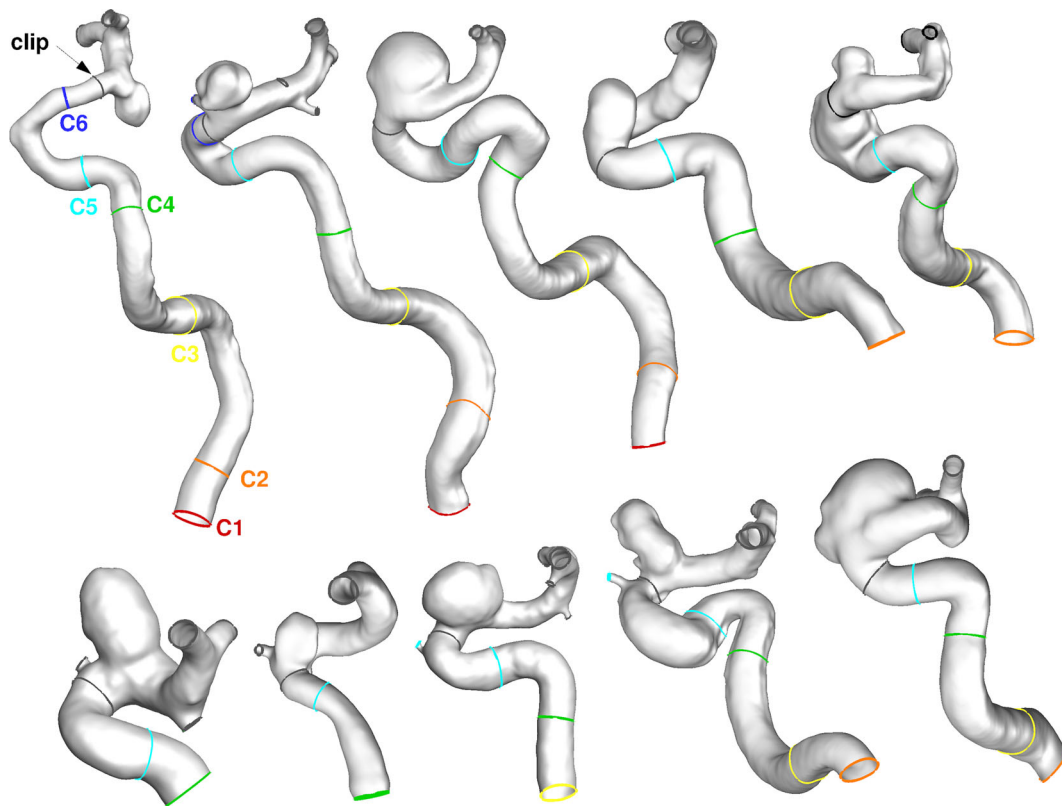


**FIGURE 1.** Representative sample of Aneurisk ICA sidewall aneurysm cases, demonstrating the variations in ICA diameter and proximal extents. Highlighted are the locations where diameters were measured, as labeled for the top left case. All cases are viewed sagittally, and shown to the same scale.

according to the convention established by Bouthillier *et al.*<sup>2</sup> These locations (C1–C7) were determined automatically as described by Piccinelli *et al.*<sup>28</sup> although in a few instances we had to manually adjust or exclude a bend point that did not correspond to C1–C7. The C1 location was excluded from the analysis because only seven of models extended that far upstream. The C7 location was excluded, as it was downstream of the aneurysm for all but one of the cases.

Cross-sectional area was computed at each location for each case, and converted to diameter under the assumption of a circular cross-section. In order to ameliorate the effects of natural or artifactual local variations in diameters, rather than take point-values at each location we averaged individual measurements over a length of two diameters, centered on the measurement point for C1–C7, or adjacent to the measurement point for Inlet and Clip locations.

#### Statistics

Unpaired t-tests using Welch's correction for unequal variances were performed to determine whether there were significant differences in measured diameters or derived flow rates, with F-tests used to

compare variances of the estimated flow rates between locations. Bland–Altman analysis was used to identify the limits of agreement for flow rates estimated from the various consistent measurement locations vs. the opportunistic (Inlet) location. Significant differences were assumed at the level of  $p < 0.05$ . All statistical analyses were performed using Prism v6.0 (Graphpad Software; San Diego, CA).

## RESULTS

Table 1 summarizes the main findings of our study. Notably, there was no significant difference in diameter until C6, where the diameter tapered by about 13% on average relative to the Inlet location ( $p < 0.003$ ). On the other hand, since flow rates were estimated based on the diameter averaged *at the particular location*, there was, as expected, no difference in average flow rate. However, variability in the estimated flow rates was significantly higher at the Clip location ( $p < 0.006$ ), reflecting the wider interindividual variability of the diameters measured there. Interindividual variabilities for flow rates estimated by the cube law ( $n = 3$ ) were also significantly higher ( $p < 0.05$ ) than those derived from a square law ( $n = 2$ ).

**TABLE 1. Descriptive statistics (mean  $\pm$  SD) for diameters (D) and flow rates (Q, in mL min<sup>-1</sup>) predicted by the flow-diameter scaling law ( $Q \sim D^n$ ) applied at the different diameter measurement locations.**

	Inlet	C2	C3	C4	C5	C6	Clip
# Cases	37	24	30	37	37	22	37
D (mm)	4.23 $\pm$ 0.52	4.24 $\pm$ 0.46	4.32 $\pm$ 0.56	4.15 $\pm$ 0.55	4.30 $\pm$ 0.60	3.70 $\pm$ 0.64	3.68 $\pm$ 0.74
Q (n = 2)	245 $\pm$ 63	245 $\pm$ 55	245 $\pm$ 64	245 $\pm$ 66	245 $\pm$ 69	245 $\pm$ 86	245 $\pm$ 101
V (cm s <sup>-1</sup> )	28.7	28.6	27.4	29.6	27.6	36.8	36.9
Q (n = 3)	245 $\pm$ 98	245 $\pm$ 84	245 $\pm$ 98	245 $\pm$ 101	245 $\pm$ 103	245 $\pm$ 134	245 $\pm$ 156
WSS (dyn cm <sup>-2</sup> )	18.4	18.5	17.2	19.3	17.4	26.3	26.0

Shown also are the resulting (fixed) cross-sectional average velocity (V) and wall shear stress (WSS) values for  $n = 2$  and  $n = 3$ , respectively.

The impact of measurement location and power law on interindividual variability of the estimated flow rates is shown more clearly in Fig. 2, where it is contextualized against ICA flow rates measured in a separate older adult population by Hoi *et al.*<sup>13</sup> It can be seen that a cube law ( $n = 3$ ) produces significantly higher variability of flow rates compared to those measured by Hoi *et al.* ( $p < 0.0002$ ), irrespective of measurement location, whereas for the square law ( $n = 2$ ), only at the Clip location was variability significantly higher than Hoi *et al.*'s ( $p < 0.0001$ ).

The impact of measurement location on flow rate estimated for individual cases using a square law is shown in Table 2. Notably, coefficients of variation ranged from less than 10% to nearly 50%, with an average of about 17%. On the other hand, and as illustrated graphically in Fig. 3, flow rates estimated from the various consistent locations vs. the opportunistic inlet location could differ for individual cases by as much as 100 mL min<sup>-1</sup> up to C5, and close to 200 mL min<sup>-1</sup> for C6 and Clip locations.

## DISCUSSION

### *Implications of Measurement Location*

Our study has demonstrated that the choice of diameter measurement location (or equivalently the model truncation site) can have a nontrivial impact on the flow rate estimated *via* scaling laws. This is important because, as noted in the Introduction, patient-specific flow rates are rarely available for aneurysm CFD studies. By the very definition of our scaling law equation, flow rates were just as likely to be overestimated as underestimated relative to the nominal population average, so however large the uncertainties might be, they would be unlikely to introduce a bias into large-scale aneurysm CFD studies. Instead, they would serve to increase the uncertainty, and hence the number of cases required to test a hypothesis to within a given power and effect size.

Coefficient of variation (CoV) in flow rate due to measurement location was found to be 17% on average, but up to nearly 50% for individual cases. While the present study did not investigate the impact of flow rate variability on downstream flow patterns, this can be inferred from other studies in the literature. For example, Cebal *et al.*<sup>5</sup> reported “changes in the velocity fields” when varying flow rates by  $\pm 25\%$  for 4 aneurysm cases (3 ICA), but noted that “characterization of the intraaneurysmal flow patterns [was] not altered”. Marzo *et al.*<sup>20</sup> reported a nearly twofold difference in flow rates measured by phase-contrast MRI in 5 aneurysm cases (3 ICA) vs. flow rates estimated assuming a fixed wall shear stress (i.e.,  $n = 3$ ) or fixed flow rate (i.e.,  $n = 0$ ). Yet, while their absolute values of WSS were evidently dependent on the choice of measured vs. assumed flow rate, their normalized WSS distributions were remarkably robust to the large discrepancies in flow rate. This is important, since large-scale aneurysm CFD studies have tended to focus on qualitative flow patterns<sup>7</sup> or normalized WSS distributions<sup>39</sup> as predictors of rupture status, suggesting that uncertainties (and indeed errors) in the estimated flow rates may be well-tolerated in clinical studies.

On the other hand, for individual case studies, large uncertainties could prove problematic. For example, per Table 2 the estimated flow rate for case C0013 was anywhere from 199 to 335 mL min<sup>-1</sup> even for the nominally uniform segment of the ICA between the C2 and C5 locations; extending to C6 and Clip locations, the estimated flow rate was as high as 515 mL min<sup>-1</sup>. Even for case C0001, which had a more typical CoV of 18%, estimated flow rates varied from 155 to 250 mL min<sup>-1</sup>, or more than 60%, which would almost certainly have a significant impact on reported absolute WSS values, if not normalized ones.

Nevertheless, it is tempting to conclude that choice of opportunistic vs. consistent diameter measurement location or truncation site is strictly irrelevant in the grand scheme of things. This would be true for vessel segments of nominally uniform caliber, such as we observed for the ICA up to C5 (mean diameter

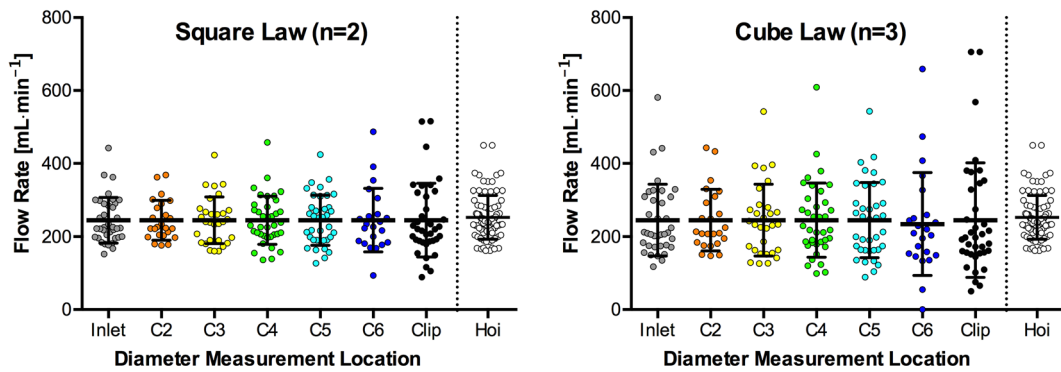


**FIGURE 2.** Distributions of flow rates estimated by square and cube scaling laws applied to each location, and compared to Hoi *et al.*'s flow rates measured in an independent cohort.<sup>13</sup> Note the consistently wider variability of data from the cube law, as expected.

**TABLE 2.** Individual flow rates (in mL min<sup>-1</sup>) estimated by the square law ( $n = 2$ ) at the different measurement locations.

Aneurisk ID	Inlet	C2	C3	C4	C5	C6	Clip	Mean	Std	CoV (%)
C0001	196	250	182	155	157	227	221	198	36	18
C0002	252	251	254	226	280	188	188	234	35	15
C0005	225	180	190	136	127	93	89	149	51	35
C0006	218	222	239	169	166	217	192	203	28	14
C0007	213	213	264	256	258	–	339	257	46	18
C0013	199	199	181	263	335	487	515	311	140	45
C0014	363	362	342	281	348	354	342	342	28	8
C0016	184	179	162	139	189	168	179	172	17	10
C0017	235	234	234	288	271	241	208	244	27	11
C0018	196	–	–	202	168	181	187	187	13	7
C0022	219	–	–	226	141	–	201	197	38	20
C0024	198	–	190	206	217	–	228	208	15	7
C0025	291	–	–	301	191	–	234	254	51	20
C0026	442	–	–	457	424	–	446	443	14	3
C0027	285	–	272	267	252	248	207	255	27	11
C0031	226	226	241	200	199	178	116	198	42	21
C0034	179	197	247	255	190	–	216	214	31	15
C0035	303	302	235	239	270	–	256	267	30	11
C0036	299	299	317	314	276	306	240	293	27	9
C0038	368	368	423	360	316	184	185	315	94	30
C0039	221	279	277	231	218	–	247	246	27	11
C0040	301	–	–	311	331	–	221	291	48	17
C0041	205	205	208	208	263	–	515	267	124	46
C0042	301	203	161	181	199	–	231	212	49	23
C0063	317	316	338	333	313	391	341	336	27	8
C0064	224	223	261	273	356	–	325	277	54	19
C0065	181	–	173	231	164	170	106	171	40	23
C0067	222	222	198	215	211	–	189	210	14	6
C0074a	200	–	–	207	227	235	142	202	37	18
C0075	177	177	183	211	256	262	154	203	42	21
C0076	280	–	268	310	280	223	193	259	43	17
C0085	153	–	–	158	190	200	201	180	23	13
C0086	252	–	241	256	212	330	320	268	46	17
C0088a	222	222	262	211	191	251	275	233	30	13
C0089	291	290	343	323	310	–	358	319	28	9
C0090	260	259	305	268	254	–	309	276	25	9
C0097	167	–	160	197	314	255	149	207	65	31

Row (intra-individual) mean, standard deviation (Std) and coefficient of variation (CoV) are shown in the rightmost columns. Column (inter-individual) statistics are shown in Table 1.

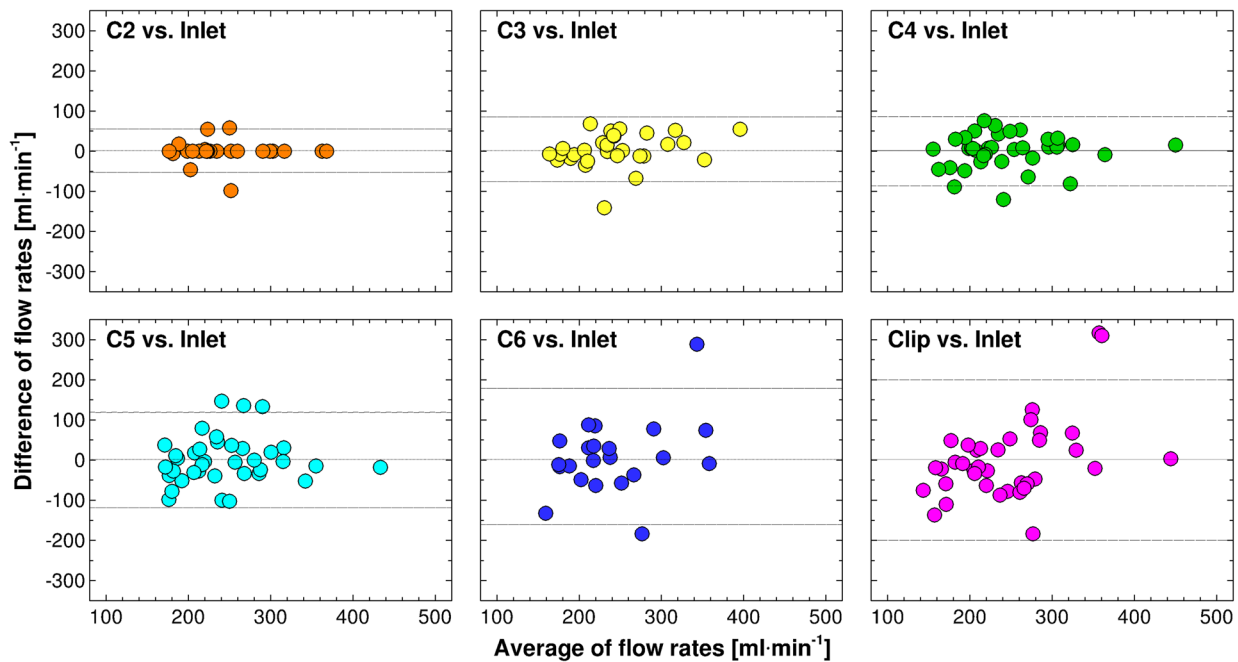


**FIGURE 3.** Bland–Altman plots reveal the non-negligible limits of agreement (upper and lower dashed lines) for individual flow rates estimated *via* square law for consistent vs. opportunistic (Inlet) locations. These highlight the dependence of a given case's estimated flow rate on where its reference diameter is measured.

4.2–4.3 mm). However, we observed a significant tapering of the ICA at C6 and Clip locations (mean diameter 3.7 mm). This is consistent with a broad survey of ICA diameters from the ISUIA study,<sup>23</sup> which indicated a tapering of the ICA from 4.2 mm at the cavernous (C4) segment to 3.8 at the communicating (C7) segment. The reduced diameter from C6 onwards is also evident from Fahrig *et al.*'s<sup>9</sup> ICA diameter of 3.5 mm based on meta-analysis of measurements made near the Circle of Willis, as well as Ingebritsen *et al.*'s<sup>14</sup> 3.6 mm at the ICA terminus. We may therefore conclude that the diameters upon which our study is based, and the reported tapering, are valid and generalize to any study focused on the ICA. Thus, choice of truncation site or diameter measurement location could matter if care is not taken to ensure that all models in a cohort consistently include the ICA proximal to C5, or that all models focus at or distal to C6. Even if such care is taken, it should be noted that failure to include a sufficient length of proximal ICA risks introducing errors in the downstream hemodynamics,<sup>10</sup> something that could only be ameliorated by direct imposition of measured velocity profiles. An indirect but potentially more serious consequence of ICA taper regards the use of published or nominal velocity or WSS values for estimating flow rates. For example, consider that for the square law ( $n = 2$ ) Table 1 shows that up to C5 the (fixed) inlet velocity came out to be around  $28 \text{ cm s}^{-1}$ , whereas distal to C5 it was  $37 \text{ cm s}^{-1}$ , a 30% increase. Such increase is con-

sistent with *in vivo* measurements: Meckel *et al.*<sup>22</sup> reported transcranial Doppler ultrasound measurements of end-diastolic velocities at C5 and C7 of  $30 \pm 0.06 \text{ cm s}^{-1}$  and  $39 \pm 0.09 \text{ cm s}^{-1}$ , respectively. This implies that velocities measured distal to the C5 location, but applied to diameters measured at or proximal to the C5 location, could uniformly underestimate flow rates by 30%. Conversely, application of ICA velocities measured proximal to C5 would serve to uniformly overestimate flow rates for models truncated at or distal to C6. Thus, it is crucial to appreciate where published *in vivo* velocity measurements are actually made.

The situation is more problematic for studies relying on the cube law ( $n = 3$ ). Again referring to Table 1, fixed WSS values came out to be around  $18 \text{ dyn cm}^{-2}$  up to C5 (assuming a viscosity of 3.5 cPoise), but increasing by nearly 50%, to  $26 \text{ dyn cm}^{-2}$  at or distal to C6. (WSS values for the square law were comparable, although by definition not fixed, e.g.,  $19.3 \pm 2.3 \text{ dyn cm}^{-2}$  at the Inlet and  $29.1 \pm 5.9 \text{ dyn cm}^{-2}$  at the Clip point.) Given that there are few and/or relatively small side branches along these segments of the ICA, this would suggest that WSS is not constant along the ICA, consistent with observations regarding intra- and inter-individual variations in WSS.<sup>8,32</sup> But it is also true that at segment C5 the ICA enters the subarachnoid space through the dural rings, which may impose constraints on vessel dimensions that have nothing to do with the principles upon which scaling laws are founded. For this reason, it would seem more logical to

estimate flow rates based on the long and uniform-diameter extradural tracts of ICA.

As a tangible example of the implications of the above arguments, consider that in a CFD study of 210 aneurysm cases, Cebal *et al.*<sup>7</sup> assumed a 15 dyn cm<sup>-2</sup> inlet WSS and a viscosity of 4 cPoise. The estimated flow rates were unfortunately not reported by those authors, but assuming their ICA cases extended proximal to C5 (e.g., assuming our Inlet diameters of 4.23 ± 0.52 mm), it would imply that they imposed ICA flow rates of only 167 ± 62 mL min<sup>-1</sup> (c.f., 245 ± 61 measured by Hoi *et al.*<sup>13</sup>). On the other hand, if based on diameters closer to C6 (e.g., assuming our Clip diameters of 3.68 ± 0.74 mm), estimated flow rates would be 110 ± 89 mL min<sup>-1</sup>, less than half the expected mean flow rate at the ICA; and WSS at the proximal inlet would be less than 10 dyn cm<sup>-2</sup>, as opposed to the intended 15 dyn cm<sup>-2</sup>.

#### *Implications of Power Law*

Our study has demonstrated that a square law ( $n = 2$ ) may be more appropriate than the popular cube law ( $n = 3$ ) for estimating ICA flow rates. The square law resulted in flow rates that demonstrably fell within a physiological range, whereas unphysiologically (or at least unlikely) high or low flow rates were evident in some cases when based on the cube law. In fact, the literature supports our observation of the suitability of a square vs. cube law at the ICA. In a study of 52 ICA terminal bifurcations, Ingebrigtsen *et al.*<sup>14</sup> reported a junction exponent of  $n = 1.7 \pm 0.8$ , whereas a cube law ( $n = 2.9 \pm 1.2$ ) was found only downstream, at the level of the (smaller) MCA bifurcation, the latter consistent also with recent measurements of MCA bifurcations by Baharoglu *et al.*<sup>1</sup> On the other hand, Cebal *et al.*<sup>6</sup> suggested that a cube law (actually  $n = 3.7$ ) was appropriate for the cerebrovasculature based on flow vs. area measurements at the ICA and vertebral arteries (VA) of 11 young adults. It is evident from those authors' plots that their nominal cube law was driven by the combination of ICA and VA data. Reanalyzing the data by separating VA and ICA measurements, we found a power law coefficient of  $n = 3.1 \pm 0.4$  for the VA and  $n = 1.8 \pm 1.0$  for the ICA. Although suggestive of cube and square laws, respectively, these power law coefficients were not statistically significantly different.

Some insight into the broader implications of the choice of power law exponent can be gleaned from Table 3. Notably, for a cube law ( $n = 3$ ), Reynolds number (Re) scales with  $D^2$ . Since normalized hemodynamic quantities essentially depend on Re, uncertainty in Re would be roughly double that of the uncertainty in the measured diameters, whereas for a

square law uncertainties in Re would be equal to uncertainties in diameter. Table 3 also includes cases where  $n = 1$  and  $n = 0$ . Use of a fixed Re ( $n = 1$ ) is relatively uncommon<sup>34</sup>; however, the assumption of a fixed flow rate ( $n = 0$ ) across a cohort is frequently made.<sup>16,30,39</sup> As Table 3 shows, a consequence of assuming a fixed flow rate is that Re (upon which, remember, normalized flow patterns most depend) scales inversely with diameter, implying, counterintuitively, that the smaller vessels in the cohort would harbor more inertial flow.

#### *Potential Limitations and Notes of Caution*

An obvious limitation of our study is that we do not know the true flow rates for our cohort, and thus can only comment on the uncertainty introduced by the choice of measurement location and power law exponent, not the accuracy of the estimated flow rates. Nevertheless, it is worth remembering that 'true' flow rates are often subject to their own measurement uncertainties or inaccuracies, as well as normal physiological variabilities, which together might serve to render them not *significantly* different from the estimated flow rates. We also did not consider the impact of pulsatile flow effects, although recent studies suggest that, at least for normalized or qualitative hemodynamic parameters, the impact of flow waveform *shape* is relatively modest.<sup>15,17,40</sup> Similar findings were reported by a study of rest vs. exercise conditions on three MCA aneurysm CFD models.<sup>3</sup> Scaling laws are also commonly used for estimating outlet flow rates or outflow divisions, investigation of which was beyond the scope of the present study. Our conclusion that the square law results in a more physiological range of flow rates also rests on the assumption that our cohort was comparable to that of Hoi *et al.*<sup>13</sup>

We did not account for the impact of small side branches or perforating vessels that would predominantly arise from C5 onwards. It may be speculated, however, that owing to their small size and/or their absence on the 3D rotational angiograms from which the Aneurisk models were derived, their impact on the assumed reference flow rate of 245 mL min<sup>-1</sup> (measured, remember, at the proximal ICA) and/or uncertainty of flow rate estimation would be negligible. We also did not explicitly account for the possibility that small side branches, if present, might have caused a slight overestimation of the (automatically-detected) vessel cross-sectional area, and hence the assumed vessel diameter. As described in the "Materials and Methods" section, in the present study we chose an averaging window of two diameters, which would likely serve to ameliorate any effects of this. In fact, we did vary the size of this window from one to four

**TABLE 3. Summary of impact of flow-diameter scaling law ( $Q \sim D^n$ ) on implied scaling of Reynolds number ( $Re$ ), cross-sectional mean velocity ( $V$ ) and wall shear stress (WSS).**

$n$	$Q$	$Re$	$V$	WSS
0	$Q = \text{const}$	$Re \sim 1/D$	$V \sim 1/D^2$	$WSS \sim 1/D^3$
1	$Q \sim D$	$Re = \text{const}$	$V \sim 1/D$	$WSS \sim 1/D^2$
2	$Q \sim D^2$	$Re \sim D$	$V = \text{const}$	$WSS \sim 1/D$
3	$Q \sim D^3$	$Re \sim D^2$	$V \sim D$	$WSS = \text{const}$

diameters, and found it to have a negligible impact on our findings except to slightly decrease (or in the case of a one-diameter window, slightly increase) the variability of the diameters and derived flow rates.

We did not explicitly investigate the impact of flow rate uncertainties on flow and WSS patterns in this cohort of cases, and thus cannot draw authoritative conclusions about the practical impact of measurement location and/or scaling law beyond the inferences we have drawn, in our Discussion above, from related studies on independent cohorts. More generally, our specific findings apply strictly to the ICA, and should be extrapolated with caution to other vessels. Having said this, the general principles regarding the impact of measurement location and power law—attention to possible systematic inconsistencies in vessel diameter (e.g., taper) and plausibility of the estimated flow rates—should be considered in any CFD simulation that relies on estimation of the boundary flow conditions.

Finally, we appreciate that actual flow rates cannot be codified into something as simplistic as a power law model. Yet it is questionable whether flow rates will ever be routinely acquired for large scale, multicenter studies. Even if they were, there is a good chance they will be based on convenient Doppler ultrasound, the accuracy of which for estimating flow has recently been questioned when there is even modest velocity profile skewing, as would be the case for larger, conduit arteries.<sup>26</sup>

### Conclusions and Recommendations

In summary, it would appear that, for the internal carotid artery at least, an opportunistic approach to estimating inlet flow rates *via* a scaling law is reasonable provided care is taken to truncate models below C5. Nevertheless, it must be recognized that the uncertainty of this approach contributes to the broader uncertainty of image-based CFD models, especially when reporting absolute as opposed to normalized hemodynamic parameters. We also recommend the use of a square law rather than the popular cube law (or indeed fixed flow or fixed  $Re$ ) to avoid potentially overestimating (or underestimating) flow and WSS dynamics for extreme cases. With this in mind, we

believe it would be of great benefit for image-based CFD studies to be more transparent about the methods used to estimate flow rates, and the values that arise from them. Such information could be readily provided as supplementary material so as not to impact often-restrictive word counts, and could provide important context as to the validity of ‘patient-specific’ simulations, as well as to guide the field towards some sort of consensus.

### ACKNOWLEDGMENTS

This study was supported by grant from the Heart & Stroke Foundation of Canada. DAS also acknowledges salary support of a Heart & Stroke Foundation Mid-Career Investigator award.

### REFERENCES

- <sup>1</sup>Baharoglu, M. I., A. Lauric, C. Wu, J. Hippelheuser, and A. M. Malek. Deviation from optimal vascular caliber control at middle cerebral artery bifurcations harboring aneurysms. *J. Biomech.* 47:3318–3324, 2014.
- <sup>2</sup>Bouthillier, A., H. R. van Loveren, and J. T. Keller. Segments of the internal carotid artery: a new classification. *Neurosurgery* 38:425–432, 1996; (discussion 432–433, 1996).
- <sup>3</sup>Bowker, T. J., P. N. Watton, P. E. Summers, J. V. Byrne, and Y. Ventikos. Rest versus exercise hemodynamics for middle cerebral artery aneurysms: a computational study. *AJNR Am. J. Neuroradiol.* 31:317–323, 2010.
- <sup>4</sup>Castro, M. A., C. M. Putman, and J. R. Cebral. Computational fluid dynamics modeling of intracranial aneurysms: effects of parent artery segmentation on intra-aneurysmal hemodynamics. *AJNR Am. J. Neuroradiol.* 27:1703–1709, 2006.
- <sup>5</sup>Cebral, J. R., M. A. Castro, S. Appanaboyina, C. M. Putman, D. Millan, and A. F. Frangi. Efficient pipeline for image-based patient-specific analysis of cerebral aneurysm hemodynamics: technique and sensitivity. *IEEE Trans. Med. Imaging* 24:457–467, 2005.
- <sup>6</sup>Cebral, J. R., M. A. Castro, C. M. Putman, and N. Alperin. Flow-area relationship in internal carotid and vertebral arteries. *Physiol. Meas.* 29:585–594, 2008.
- <sup>7</sup>Cebral, J. R., F. Mut, J. Weir, and C. M. Putman. Association of hemodynamic characteristics and cerebral aneurysm rupture. *AJNR Am. J. Neuroradiol.* 32:264–270, 2011.



- <sup>8</sup>Cheng, C., F. Helderma, D. Tempel, D. Segers, B. Hierck, R. Poelmann, A. van Tol, D. J. Duncker, D. Robbers-Visser, N. T. C. Ursem, R. van Haperen, J. J. Wentzel, F. Gijzen, A. F. W. van der Steen, R. de Crom, and R. Krams. Large variations in absolute wall shear stress levels within one species and between species. *Atherosclerosis*. 195:225–235, 2007.
- <sup>9</sup>Fahrig, R., H. Nikolov, A. J. Fox, and D. W. Holdsworth. A three-dimensional cerebrovascular flow phantom. *Med. Phys.* 26:1589–1599, 1999.
- <sup>10</sup>Hodis, S., S. Kargar, D. F. Kallmes, and D. Dragomir-Daescu. Artery length sensitivity in patient-specific cerebral aneurysm simulations. *AJNR Am. J. Neuroradiol.* 2014. doi:10.3174/ajnr.A4179.
- <sup>11</sup>Hoi, Y., B. A. Wasserman, E. G. Lakatta, and D. A. Steinman. Carotid bifurcation hemodynamics in older adults: effect of measured versus assumed flow waveform. *J. Biomech. Eng.* 132:071006, 2010.
- <sup>12</sup>Hoi, Y., B. A. Wasserman, E. G. Lakatta, and D. A. Steinman. Effect of common carotid artery inlet length on normal carotid bifurcation hemodynamics. *J. Biomech. Eng.* 132:121008, 2010.
- <sup>13</sup>Hoi, Y., B. A. Wasserman, Y. J. Xie, S. S. Najjar, L. Ferruci, E. G. Lakatta, G. Gerstenblith, and D. A. Steinman. Characterization of volumetric flow rate waveforms at the carotid bifurcations of older adults. *Physiol. Meas.* 31:291–302, 2010.
- <sup>14</sup>Ingebrigtsen, T., M. K. Morgan, K. Faulder, L. Ingebrigtsen, T. Sparr, and H. Schirmer. Bifurcation geometry and the presence of cerebral artery aneurysms. *J. Neurosurg.* 101:108–113, 2004.
- <sup>15</sup>Jansen, I. G., J. J. Schneiders, W. V. Potters, P. van Ooij, R. van den Berg, E. van Bavel, H. A. Marquering, and C. B. Majoie. Generalized versus patient-specific inflow boundary conditions in computational fluid dynamics simulations of cerebral aneurysmal hemodynamics. *AJNR Am. J. Neuroradiol.* 35:1543–1548, 2014.
- <sup>16</sup>Jou, L. D., D. H. Lee, H. Morsi, and M. E. Mawad. Wall shear stress on ruptured and unruptured intracranial aneurysms at the internal carotid artery. *AJNR Am. J. Neuroradiol.* 29:1761–1767, 2008.
- <sup>17</sup>Karmonik, C., C. Yen, O. Diaz, R. Klucznik, R. G. Grossman, and G. Benndorf. Temporal variations of wall shear stress parameters in intracranial aneurysms—importance of patient-specific inflow waveforms for CFD calculations. *Acta Neurochir.* 152:1391–1398, 2010; (discussion 1398, 2010).
- <sup>18</sup>Langille, B. L., and F. O'Donnell. Reductions in arterial diameter produced by chronic decreases in blood flow are endothelium-dependent. *Science* 231:405–407, 1986.
- <sup>19</sup>Lee, S. W., L. Antiga, J. D. Spence, and D. A. Steinman. Geometry of the carotid bifurcation predicts its exposure to disturbed flow. *Stroke* 39:2341–2347, 2008.
- <sup>20</sup>Marzo, A., P. Singh, I. Larrabide, A. Radaelli, S. Coley, M. Gwilliam, I. D. Wilkinson, P. Lawford, P. Reymond, U. Patel, A. Frangi, and D. R. Hose. Computational hemodynamics in cerebral aneurysms: the effects of modeled versus measured boundary conditions. *Ann. Biomed. Eng.* 39:884–896, 2011.
- <sup>21</sup>Marzo, A., P. Singh, P. Reymond, N. Stergiopoulos, U. Patel, and R. Hose. Influence of inlet boundary conditions on the local haemodynamics of intracranial aneurysms. *Comput. Methods Biomech. Biomed. Eng.* 12:431–444, 2009.
- <sup>22</sup>Meckel, S., L. Leitner, L. H. Bonati, F. Santini, T. Schubert, A. F. Stalder, P. Lyrer, M. Markl, and S. G. Wetzel. Intracranial artery velocity measurement using 4D PC MRI at 3 T: comparison with transcranial ultrasound techniques and 2D PC MRI. *Neuroradiology* 55:389–398, 2013.
- <sup>23</sup>Mocco, J., J. Huston, K. M. Fargen, J. Torner, and R. D. Brown, Jr. An angiographic atlas of intracranial arterial diameters associated with cerebral aneurysms. *J. Neurointerv. Surg.* 6:533–535, 2014.
- <sup>24</sup>Morbiducci, U., R. Ponzini, D. Gallo, C. Bignardi, and G. Rizzo. Inflow boundary conditions for image-based computational hemodynamics: impact of idealized versus measured velocity profiles in the human aorta. *J. Biomech.* 46:102–109, 2013.
- <sup>25</sup>Murray, C. D. The physiological principle of minimum work: I. The vascular system and the cost of blood volume. *Proc. Natl. Acad. Sci. USA* 12:207–214, 1926.
- <sup>26</sup>Mynard, J. P., and D. A. Steinman. Effect of velocity profile skewing on blood velocity and volume flow waveforms derived from maximum Doppler spectral velocity. *Ultrasound Med. Biol.* 39:870–881, 2013.
- <sup>27</sup>Pereira, V. M., O. Brina, and A. Marcos. Gonzales, A. P. Narata, P. Bijlenga, K. Schaller, K. O. Lovblad, and R. Ouared. Evaluation of the influence of inlet boundary conditions on computational fluid dynamics for intracranial aneurysms: a virtual experiment. *J. Biomech.* 46:1531–1539, 2013.
- <sup>28</sup>Piccinelli, M., S. Bacigaluppi, E. Boccardi, B. Ene-Iordache, A. Remuzzi, A. Veneziani, and L. Antiga. Geometry of the internal carotid artery and recurrent patterns in location, orientation, and rupture status of lateral aneurysms: an image-based computational study. *Neurosurgery*. 68:1270–1285, 2011; (discussion 1285, 2011).
- <sup>29</sup>Piccinelli, M., D. A. Steinman, Y. Hoi, F. Tong, A. Veneziani, and L. Antiga. Automatic neck plane detection and 3D geometric characterization of aneurysmal sacs. *Ann. Biomed. Eng.* 40:2188–2211, 2012.
- <sup>30</sup>Qian, Y., H. Takao, M. Umezumi, and Y. Murayama. Risk analysis of unruptured aneurysms using computational fluid dynamics technology: preliminary results. *AJNR Am. J. Neuroradiol.* 32:1948–1955, 2011.
- <sup>31</sup>Sangalli, L. M., P. Secchi, S. Vantini, and A. Veneziani. A case study in exploratory functional data analysis: geometrical features of the internal carotid artery. *J. Am. Stat. Assoc.* 104:37–48, 2009.
- <sup>32</sup>Stroev, P. V., P. R. Hoskins, and W. J. Eason. Distribution of wall shear rate throughout the arterial tree: a case study. *Atherosclerosis*. 191:276–280, 2007.
- <sup>33</sup>Taylor, C. A., and D. A. Steinman. Image-based modeling of blood flow and vessel wall dynamics: applications, methods and future directions. *Ann. Biomed. Eng.* 38:1188–1203, 2010.
- <sup>34</sup>Tremmel, M., S. Dhar, E. I. Levy, J. Mocco, and H. Meng. Influence of intracranial aneurysm-to-parent vessel size ratio on hemodynamics and implication for rupture: results from a virtual experimental study. *Neurosurgery*. 64:622–630, 2009; (discussion 630–631, 2009).
- <sup>35</sup>Valen-Sendstad, K., M. Piccinelli, and D. A. Steinman. High-resolution computational fluid dynamics detects flow instabilities in the carotid siphon: implications for aneurysm initiation and rupture? *J. Biomech.* 47:3210–3216, 2014.
- <sup>36</sup>Valen-Sendstad, K., and D. A. Steinman. Mind the gap: impact of computational fluid dynamics solution strategy on prediction of intracranial aneurysm hemodynamics and rupture status indicators. *AJNR Am. J. Neuroradiol.* 35:536–543, 2014.

- <sup>37</sup>Wake, A. K., J. N. Oshinski, A. R. Tannenbaum, and D. P. Giddens. Choice of in vivo versus idealized velocity boundary conditions influences physiologically relevant flow patterns in a subject-specific simulation of flow in the human carotid bifurcation. *J. Biomech. Eng.* 131:021013, 2009.
- <sup>38</sup>Weinberg, P., and C. R. Ethier. Twenty-fold difference in hemodynamic wall shear stress between murine and human aortas. *J. Biomech.* 40:1594–1598, 2007.
- <sup>39</sup>Xiang, J., S. K. Natarajan, M. Tremmel, D. Ma, J. Mocco, L. N. Hopkins, A. H. Siddiqui, E. I. Levy, and H. Meng. Hemodynamic-morphologic discriminants for intracranial aneurysm rupture. *Stroke* 42:144–152, 2011.
- <sup>40</sup>Xiang, J., A. H. Siddiqui, and H. Meng. The effect of inlet waveforms on computational hemodynamics of patient-specific intracranial aneurysms. *J. Biomech.* 47:3882–3890, 2014.
- <sup>41</sup>Zamir, M., P. Sinclair, and T. H. Wonnacott. Relation between diameter and flow in major branches of the arch of the aorta. *J. Biomech.* 25:1303–1310, 1992.